RAA 2014 Vol. **14** No. **6**, 741–752 doi: 10.1088/1674–4527/14/6/012
http://www.raa-journal.org *http://www.iop.org/journals/raa*

Research in Astronomy and Astrophysics

Evolution of isolated G-band bright points: size, intensity and velocity *

Yun-Fei Yang[1,2,3], Jia-Ben Lin[2], Song Feng[1,2,3], Kai-Fan Ji[1], Hui Deng[1] and Feng Wang[1]

[1] Faculty of Information Engineering and Automation / Yunnan Key Laboratory of Computer Technology Application, Kunming University of Science and Technology, Kunming 650500, China; *yfyangkmust@gmail.com*
[2] Key Laboratory of Solar Activity, National Astronomical Observatories, Chinese Academy of Sciences, Beijing 100012, China
[3] Key Laboratory of Modern Astronomy and Astrophysics, Nanjing University, Ministry of Education, Nanjing 210093, China

Received 2013 October 10; accepted 2013 December 3

Abstract We study the evolution pattern of isolated G-band bright points (GBPs) in terms of their size, intensity and velocity. Using a high resolution image sequence taken with the Hinode/Solar Optical Telescope (SOT), we detect GBPs in each image by the Laplacian and Morphological Dilation algorithm, and track their evolutions by a 26-adjacent method in a three-dimensional space-time cube. For quantifying the evolution, we propose a quantification method based on lifetime normalization which aligns the different lifetimes to common stages. The quantification results show that, on average, the diameter of isolated GBPs changes from 166 to 173 km, then down to 165 km; the maximum intensity contrast changes from 1.012 to 1.027, then down to 1.011; however, the velocity changes from 1.709 to 1.593 km s^{-1}, then up to 1.703 km s^{-1}. The results indicate that the evolution follows a pattern such that the GBP is small, faint and fast-moving at the birth stage, becomes big, bright and slow-moving at the middle stage, then gets small, faint and fast-moving at the decay stage until disappearance. Although the differences are very small, a two-sample t-test is used to demonstrate there are significant differences in means between the distributions of the different stages. Furthermore, we quantify the relationship between the lifetimes of GBPs and their properties. It is found that there are positive correlations between the lifetimes and their sizes and intensities with correlation coefficients of 0.83 and 0.65, respectively; however, there is a negative correlation between the lifetimes and velocities with a correlation coefficient of –0.49. In summary, the longer the GBP persists, the bigger, brighter and slower it will be.

Key words: techniques: image processing — Sun: photosphere — methods: data analysis — methods: statistical

* Supported by the National Natural Science Foundation of China.

1 INTRODUCTION

Some tiny bright structures located in the intergranular dark lanes are very clearly seen in G-band images of the solar photosphere. They form filigrees, flowers and some other shapes. In this paper, we call them G-band bright points (GBPs). These GBPs arise from small scale active events on the Sun, and their motions are thought to be the ultimate energy source for heating the chromosphere and corona and accelerating the solar wind, either via waves or via magnetic reconnection of intertwined flux tubes (Cranmer 2002; Cranmer & van Ballegooien 2005; Klimchuk 2006, Zhao et al. 2009).

The statistics describing their properties, such as size, intensity, velocity and lifetime, have been studied during recent years. A typical diameter of a GBP is 100–300 km (Berger et al. 1995; Bovelet et al. 2003; Sánchez Almeida et al. 2004; Utz et al. 2009; Crockett et al. 2010; Feng et al. 2012a; Feng et al. 2013). The ratio of the maximum intensity of a GBP to its mean photospheric intensity is 0.8–1.8 (Berger et al. 1995; Sánchez Almeida et al. 2004). The mean horizontal velocity is approximately 1–2 km s^{-1} with a maximum value of 7 km s^{-1} (Muller et al. 1994; Berger et al. 1998; Utz et. al 2009; Keys et al. 2011; Feng et al. 2013; Keys et al. 2013). The mean lifetime is 2–10 min (Berger et al. 1998; Nisenson et al. 2003; Sánchez Almeida et al. 2004; de Wijn et al. 2005; Möstl et al. 2006; Utz et al. 2010).

However, studies focusing on evolution of the GBPs in terms of their properties are relatively scarce. Muller et al. (1992) reported that a small bright point appeared; after a few minutes, the bright point reached its maximum visibility; as the granules evolved, the bright point slowly faded. Utz et al. (2009) also mentioned the bright point was weak at the beginning and decayed. Except for those cases, the evolution of their size and velocity has seldom been mentioned.

In this paper, using the G-band high resolution image sequence with the Solar Optical Telescope (SOT; Ichimoto et al. 2004; Suematsu et al. 2008) onboard Hinode, we concentrate on quantifying the evolution of isolated GBPs in terms of their size, intensity and velocity, to explore their evolution pattern.

Furthermore, we quantify the relationship between their lifetimes and properties. The layout of the paper is as follows. The observations and data reduction are described in Section 2. The method used to track GBPs is discussed in Section 3. The quantification method and main findings of the evolution are presented in Section 4. The relationships between their lifetimes and properties are analyzed in Section 5. Finally, the discussion and conclusion are given in Sections 6 and 7 respectively.

2 OBSERVATIONS AND DATA REDUCTION

In order to minimize the deleterious effects of bad seeing conditions and image reconstruction from ground-based observations, the data acquired from space with high resolution offer an excellent opportunity for systematic statistical studies of small scale dynamic motions.

The data used in this study were obtained with the SOT onboard the Hinode satellite in the G-band with wavelengths of 430.5 nm, taken between 18:19 UT and 20:40 UT on 2007 February 19. The SOT has a 0.5 m aperture with a diffraction-limited spatial resolution of $0.22''$. The field of view (FOV) is $27.7'' \times 27.7''$ in a quiet region at the center of the solar disk with a pixel size of $0.054''$. The data sequence consists of 758 exposures over a period of roughly 2 h and 20 min with a cadence of 11 s. The level-0 sequence is calibrated and reduced to level-1 using the standard data reduction algorithm fg_prep.pro distributed in solar software.

Furthermore, the calibrated sequence is carefully aligned at the sub-pixel level by a measurement of the centroid on the cross correlation surface with the modified moment method (Feng et al. 2012b) for correcting satellite drift. The aligned FOV is $20.5'' \times 20.5''$ (380 pixel$\times$380 pixel) and 758 frames have been de-stretched.

3 TRACKING GBPS

In order to track the evolution of GBPs, the GBPs first need to be detected and identified in every image. Therefore, we use a Laplacian and Morphological Dilation algorithm, described in Feng et al. (2012a, 2013), and detect a total of 29 092 GBPs in 758 images. After that, we further apply the algorithm to track the evolution of GBPs in the image sequence.

According to previous research, GBPs have a typical diameter of 100–300 km, and a maximum horizontal velocity of 7 km s^{-1}. With a cadence of 11 s, the displacement of an individual GBP between two successive frames will be limited to 77 km, which means it is limited to the size of one GBP. In other words, if we observe the projection of a GBP on a time-slice, the projections of a GBP in two successive frames should be overlapped or adjoined. Thus, we model the detected GBPs in 758 images as a three dimensional (3D) space-time cube (x, y and z) such that the x and y axes are the two dimensional image coordinates, and the z axis represents a frame index or time-slice of the image sequence. Fortunately, 3D image processing methods can help us track GBPs in the 3D space-time cube, in particular the 26-adjacent technique. Consider that p and q are two voxels in Z^3 denoted by $p = (p_x, p_y, p_z)$ and $q = (q_x, q_y, q_z)$. The p and q are called 26-adjacent if $|p_x - q_x| \leq 1$, $|p_y - q_y| \leq 1$ and $|p_z - q_z| \leq 1$. A 26-adjacent is like a Rubik's Cube in which the center voxel is adjacent to neighboring voxels in 26 directions. The connected voxels in the 3D space-time cube which satisfy the 26-adjacent condition are then labeled by a unique index, and regarded as an individual 3D structure. The 3D structure represents the process of evolution for the GBP, so we call it a 3D evolutional structure. After applying the 26-adjacent routine to the 3D space-time cube, the 29 092 detected GBPs are labeled, yielding a total of 2778 3D evolutional structures.

An isolated GBP can be easily distinguished from the 3D evolutional structures. It is defined such that no merging or splitting events occur during its life. Therefore, a 3D evolutional structure corresponds to the evolution of an isolated GBP if there is only one individual region in each frame (time-slice), and it has the form of a cylindrical tube. Figure 1(a) shows the process of evolution as a sequence of images for an isolated GBP which persists in 27 successive frames. Only nine frames are shown here.

Figure 1(b) shows the cylindrical tube that corresponds to the evolution of the GBP in Figure 1(a) in the 3D space-time cube. Compared to the sequence of images, the 3D evolutional structure highlights the evolution of a GBP in a single figure. In addition, we could obtain the properties of GBP intuitively. For instance, the lifetime could be calculated by the length of a 3D evolutional structure in the time dimension; the change in shape and size during its life can be represented as an irregular cylinder; the velocity of a GBP can be calculated by the displacement of a centroid between successive frames of the 3D evolutional structure.

On the other hand, a non-isolated GBP is defined such that one GBP merges with other GBPs or one GBP splits into two or more GBPs, forming a very complex structure in the 3D space-time cube. In the following study, we only focus on isolated GBPs to explore their evolution pattern. This is because their lifetime, size, intensity and velocity are clearly defined, and 2596 isolated 3D evolutional structures account for 93% of all images in this sequence.

Thus far, we have obtained the properties of isolated GBPs, like lifetime, equivalent diameter (the circular shape covering its area), intensity and velocity. For reducing the chances of measuring structures that represent noise, an isolated GBP would be discarded if it meets any of the conditions described as follows: (1) it only exists in a single image; (2) its equivalent diameter is smaller than 100 km, because the diffraction-limited spatial resolution of the SOT is $0.22''$; (3) its equivalent diameter is larger than 300 km, because two or more isolated GBPs are adjacent from the beginning to end of the sequence; (4) its life cycle is not complete, for instance, the GBP is located at the border of an image, and the GBP starts at the first frame or ends at the last frame. As a result, a total of 12 457 GBPs remain and are labeled, yielding a total of 1786 3D evolutional structures.

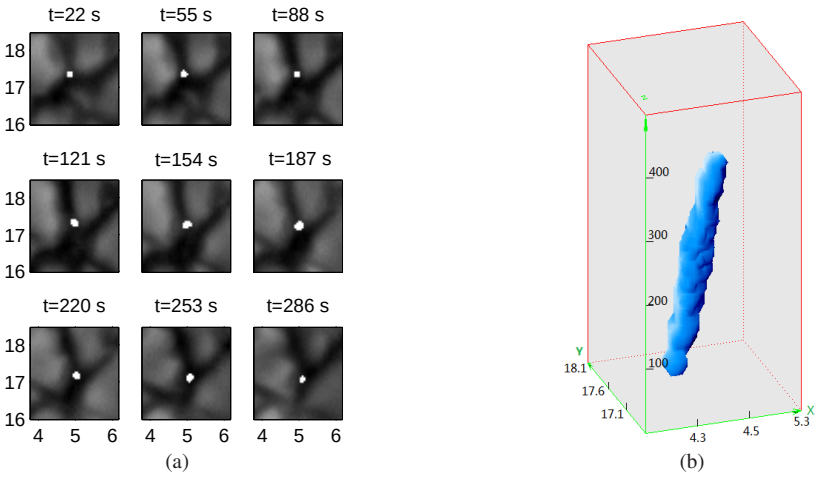

(a) (b)

Fig. 1 The evolution of an isolated GBP. (a) shows a detected, isolated GBP marked in white in the image sequence. The sequence starts at the upper left and ends at the lower right. Positions are given in arcsec from the bottom left corner of the full frame. (b) shows the cylindrical tube corresponding to the GBP in (a) in the 3D space-time cube. The X and Y axes are ticked in arcsec, and the Z axis is ticked in seconds.

Before quantifying the evolution of isolated GBPs in terms of their properties, we analyze the statistical distributions and calculate the mean values of these properties. The probability density function (PDF) of lifetime fits the curve of an exponential distribution well, with mathematical expectation of 2.56 ± 0.35 min. The equivalent diameter is used for analyzing the size of GBPs, and fitting a normal distribution is more suitable for the PDF with $= 170$ km (mean) and $= 46$ km (standard deviation). The maximum intensity contrast is defined as a ratio of the maximum intensity of the GBP to the mean photospheric intensity for analyzing the intensity of GBPs, and the PDF of the maximum intensity contrast is fitted with a normal distribution very well with $\mu = 1.02$ and $\sigma = 0.11$. The velocity is calculated by the displacement of the centroid between two successive frames. The PDFs of velocities in the x direction, v_x, and the y direction, v_y, are fitted by a normal distribution with $\mu = -0.01\,\mathrm{km\ s^{-1}}$ and $\sigma = 1.40\ \mathrm{km\ s^{-1}}$ for v_x, and $\mu = 0.03\,\mathrm{km\ s^{-1}}$ and $\sigma = 1.38\,\mathrm{km\ s^{-1}}$ for v_y. Both of the means are close to 0, which also implies the image sequence has been precisely aligned. The velocity is then calculated by the equation $v = \sqrt{v_x^2 + v_y^2}$. The PDF of velocity is Rayleigh fitted with mathematical expectation of $1.66 \pm 0.1\,\mathrm{km\ s^{-1}}$. These results all agree with previous studies.

4 QUANTIFYING THE EVOLUTION OF ISOLATED GBPS

4.1 Method used for Quantification

Our purpose is to quantify the process of evolution that occurs in isolated GBPs in terms of their properties, such as diameter, intensity and velocity. The basis of the quantification method is lifetime normalization which standardizes different lifetimes to common stages. The lifetimes of isolated GBPs vary from 11 s to 17.97 min (from 2 to 99 successive frames) in this image sequence. No matter how long the lifetime is, we divide the life of a GBP into common stages, then calculate the mean values of properties associated with different stages. However, it is impossible to divide the life of GBPs which persist on less than N frames into N stages (given N is the number of common

stages). Besides that, it is meaningless to explore properties of the evolution pattern for short-lived GBPs. Therefore, we only use isolated GBPs which persist on at least N frames when we divide the life into N stages. A quantification method consisting of the following steps is developed:

(1) Select isolated GBPs which persist on at least N successive frames.
(2) Divide the life of each isolated GBP into N stages. Mathematically, given that a GBP persists on Lt frames, the number of frames covering one stage can be calculated as

$$Fn = Lt/N. \tag{1}$$

If Lt cannot be divided by N, the remaining frames after the division are regarded as the last stage.
(3) Calculate the arithmetic mean MS_i (where $i = 1-N$ denotes the different stages) for properties of GBPs at each stage. This step is repeated for each GBP. Consequently, each GBP has N mean values representing the process of evolution at N stages.
(4) Normalize the MS_i by the following formula

$$MR_i = MS_i/MG \qquad (i = 1 - N), \tag{2}$$

where MG is the mean value of a property associated with a GBP during its whole life. MR_i is the ratio between the mean value at stage i and the mean value of this GBP. For instance, the diameter ratio is the ratio between the mean diameter of each stage and the mean diameter of this GBP. The intensity ratio, the velocity ratio and so on are calculated in a similar way.
(5) Divide the ratios (MR_i) of all GBPs into N groups at different stages, or the ratios at the same stage can be divided into one group, and then the PDFs of the ratios can be separately curve fitted for each group. By using the distribution functions, the means of the ratios, the lower and upper bounds of the confidence intervals for the means and the standard deviations at N stages are obtained.
(6) Plot the values and error bars using the means of the ratios and the bounds of the confidence intervals for the means of N stages, to illustrate the evolution pattern of properties associated with isolated GBPs.

In general, dividing the life into five stages is representative of the entire evolution process, which can be described as birth, growth, middle, decay and disappearance. Each stage covers 20% of the entire life. To perform this analysis, a total of 905 isolated GBPs which persist on at least five frames are selected, and their lives are divided into five stages. To compare results of these five stages, we also select a total of 416 GBPs which persist on at least 10 frames, divide their lives into 10 stages and apply the same method. The results of quantification for the diameter, maximum intensity contrast and velocity of isolated GBPs are analyzed in the following.

4.2 The Diameter

The PDFs of the diameter ratios are each curve fitted for five stages and all of them are adequately described by a normal distribution. Therefore, the means of the diameter ratios, the bounds of the confidence intervals for the means and the standard deviations of five stages are calculated. Due to the mean diameter being 170 km, we also calculate the corresponding diameter by multiplying the mean of the ratio and the mean diameter.

Table 1 shows the results of calculating the diameter at the five different stages. Using the means of the ratios and bounds of the confidence intervals for the means, we plot the values and associated error bars in Figure 2(a). It can be seen that the evolution pattern for size is that the size of an isolated GBP is small at birth, then it continues to increase; at the middle stage, it reaches its peak, then decreases in the decay stage until disappearance. The result agrees with the deformation of the

Table 1 Results of the Diameter of GBPs by Dividing their Lives into Five Stages

Stage	Mean of diameter ratio	Bound	Standard deviation	Diameter (km)
Birth	0.977	±0.0074	0.1136	166
Growth	1.01	±0.0051	0.0779	171
Middle	1.021	±0.0043	0.0657	173
Decay	1.00	±0.0051	0.0784	170
Disappearance	0.973	±0.0077	0.1179	165

Table 2 Results of the Diameter of GBPs by Dividing their Lives into 10 Stages

Stage	Mean of diameter ratio	Bound	Standard deviation	Diameter (km)
1	0.951	±0.0111	0.1151	161
2	0.998	±0.0094	0.0976	169
3	1.015	±0.0083	0.0864	172
4	1.018	±0.0072	0.0752	173
5	1.019	±0.0073	0.0761	173
6	1.023	±0.0073	0.0757	174
7	1.017	±0.0070	0.0732	172
8	1.006	±0.0084	0.0878	171
9	0.997	±0.0100	0.1038	169
10	0.953	±0.0125	0.1298	162

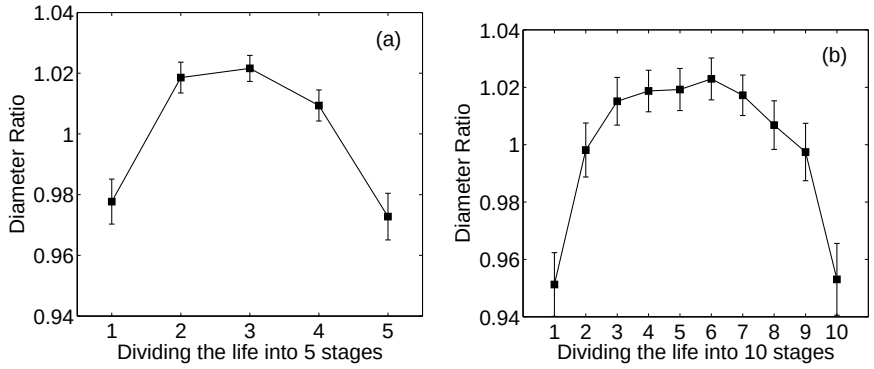

Fig. 2 The evolution of the size of GBPs. The diameter ratio is the mean diameter at each stage normalized by the mean diameter of this GBP. The values with error bars show the variation of diameter by dividing the life into five stages (a) and 10 stages (b).

GBP shown in Figure 1(b). In fact, the diameter of that GBP is 134 km in the birth stage, and rises until its peak of 195 km at the middle stage, then decreases to 141 km just before disappearing.

We apply the quantification algorithm by again dividing the life into 10 stages. The quantification results are shown in Table 2 and are plotted with error bars in Figure 2(b). The mean of the diameter ratio is 0.951 at the first stage, and it increases to its peak of 1.023 at the sixth stage, then decreases to 0.953 at the last stage. The results in Table 2 are similar to those in Table 1, and the pattern of values plotted in Figure 2(b) agrees with that in Figure 2(a), except that the difference between the maximum and minimum value (0.072) in Figure 2(b) is higher than that (0.048) in Figure 2(a).

Table 3 Results of the Intensity of GBPs by Dividing their Lives into Five Stages

Stage	Mean of intensity ratio	Bound	Standard deviation	Maximum intensity contrast
Birth	0.993	±0.0030	0.0463	1.012
Growth	1.005	±0.0020	0.0314	1.025
Middle	1.007	±0.0017	0.0267	1.027
Decay	1.002	±0.0020	0.0307	1.022
Disappearance	0.992	±0.0028	0.0433	1.011

Table 4 Results of the Intensity of GBPs by Dividing their Lives into 10 Stages

Stage	Mean of intensity ratio	Bound	Standard deviation	Maximum intensity contrast
1	0.979	±0.0056	0.0590	0.998
2	0.996	±0.0045	0.0476	1.015
3	1.006	±0.0040	0.0420	1.026
4	1.011	±0.0041	0.0426	1.031
5	1.010	±0.0039	0.0405	1.030
6	1.009	±0.0035	0.0367	1.029
7	1.006	±0.0036	0.0382	1.026
8	1.002	±0.0039	0.0410	1.022
9	0.994	±0.0044	0.0462	1.013
10	0.982	±0.0052	0.0545	1.001

4.3 The Maximum Intensity Contrast

Dividing the life into five stages, the PDFs of the intensity ratios for each stage are curve fitted separately and all of them follow a normal distribution. Due to the mean maximum intensity contrast being 1.02, we also calculate the corresponding maximum intensity contrast by multiplying the mean ratio and mean maximum intensity contrast.

Table 3 shows the quantification result of the maximum intensity contrast by dividing the life into five stages and the values are plotted with error bars in Figure 3(a). It can also be seen that the evolution pattern of intensity is that the isolated GBP is faint at birth, then becomes bright until its peak at the middle stage, and fades away at the decay stage until disappearance. The result also agrees with the GBP shown in Figure 1(b). In fact, the maximum intensity contrast of that GBP in Figure 1(b) is 1.02 at the birth stage, and it increases to 1.14 at the middle stage, then decreases to 0.91 until the disappearance.

The quantification results of dividing the life into 10 stages are shown in Table 4 and the values and associated error bars are in Figure 3(b). The mean of the intensity ratio is 0.979 at the first stage, and it increases to its peak of 1.011 at the fourth stage, then decreases to 0.982 at the last stage. These results coincide with Table 3 and Figure 3(a). Like the diameter, the difference between the maximum and minimum value (0.032) of 10 stages is also higher than that (0.015) of five stages.

4.4 The Velocity

The PDFs of the velocity ratios in five stages are each separately fitted to a Rayleigh distribution. The quantification results are shown in Table 5 and the values with associated error bars are plotted in Figure 4(a). According to the mean velocity of 1.66 km s^{-1}, the corresponding velocity is calculated. In contrast to the size and intensity, both Table 5 and Figure 4(a) show that the velocity ratio is high in the birth and disappearance stages, but low in the middle stage. It can be seen that the evolution pattern of velocity shows exactly the opposite trend: an isolated GBP moves fast at birth, then decreases to its lowest value in the middle stage, and speeds up in the decay stage until disappearance.

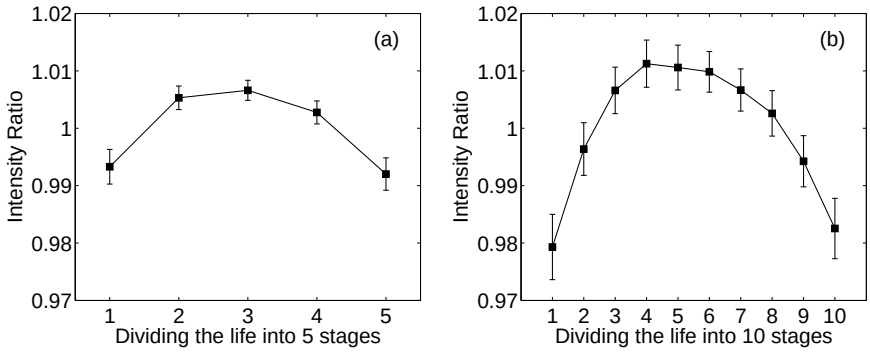

Fig. 3 The evolution of intensity ratio for the GBPs. The intensity ratio is the mean maximum intensity contrast at each stage normalized by the mean of this GBP. The values are plotted with error bars and show the variation of intensity ratio by dividing the life into five stages (a) 10 stages (b).

Table 5 Results of the Velocity of GBPs by Dividing their Lives into Five Stages

Stage	Mean of velocity ratio	Bound	Standard deviation	Velocity (km s^{-1})
Birth	1.034	±0.0318	0.3993	1.709
Growth	0.974	±0.0293	0.3687	1.616
Middle	0.960	±0.0310	0.3891	1.593
Decay	1.003	±0.0334	0.4197	1.665
Disappearance	1.026	±0.0346	0.4348	1.703

Table 6 Results for Velocity of GBPs by Dividing their Lives into 10 Stages

Stage	Mean of velocity ratio	Bound	Standard deviation	Velocity (km s^{-1})
1	1.086	±0.0497	0.435	1.802
2	0.994	±0.0487	0.427	1.650
3	0.965	±0.0495	0.434	1.602
4	0.963	±0.0423	0.370	1.598
5	0.940	±0.0419	0.367	1.560
6	0.954	±0.0449	0.393	1.584
7	0.990	±0.0471	0.412	1.643
8	0.991	±0.0529	0.463	1.645
9	0.995	±0.0558	0.488	1.652
10	1.123	±0.0602	0.527	1.864

Table 6 shows the quantification result of dividing the life into 10 stages and Figure 4(b) shows the values with error bars which correspond to Figure 4(a). It can be seen that the evolution pattern of the 10 stages agrees with that of the five stages. However, the means of velocity ratios of 10 stages change from 1.086 to 0.940, then up to 1.123. Like the the diameter and intensity, the difference between the maximum and minimum value (0.183) of 10 stages is higher than that (0.074) of five stages.

5 THE RELATIONSHIP BETWEEN THE LIFETIMES AND PROPERTIES

We are also interested in the relationship between lifetimes of isolated GBPs and their properties. Among the total of 1786 isolated GBPs, we ignore the 0.5% of GBPs (9 GBPs) which live more than 10 min. The lifetime of one GBP is calculated according to the number of successive frames on which the GBP persists. Since the cadence is 11 s, the lifetimes of 1777 isolated GBPs that persist

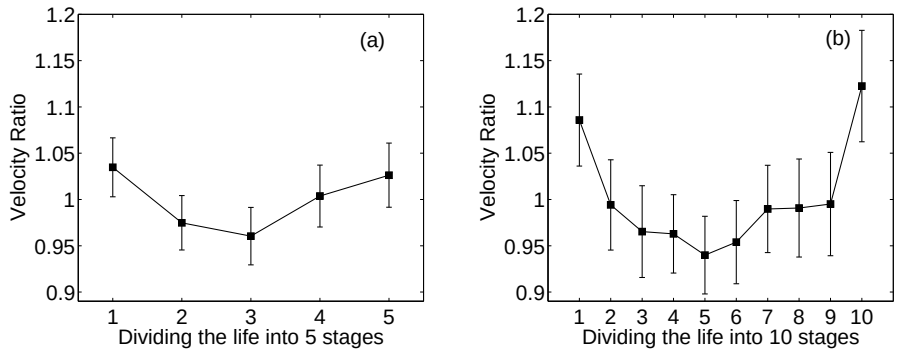

Fig. 4 The evolution velocity of the GBPs. The velocity ratio is the mean velocity at each stage normalized by the mean of this GBP. The error bar shows the variation of velocity by dividing the life into five stages (a) and 10 stages (b).

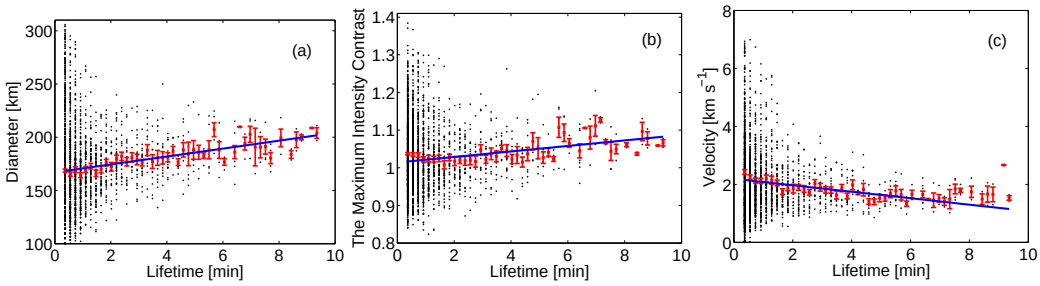

Fig. 5 The lifetimes of isolated GBPs are plotted versus their diameters (a), the maximum intensity contrasts (b) and velocities (c). The error bars show the means and their standard errors calculated for each different lifetime. Straight solid lines are the best linear fit for the means of error bars.

from 2 to 55 successive frames vary from 11 s to 10 min. In our data set, 46 different lifetimes are identified. The scatter associated with the lifetimes of 1777 isolated GBPs versus their other properties, such as diameters, the maximum intensity contrasts and velocities are shown in black in Figure 5(a), Figure 5(b) and Figure 5(c), respectively. Then, we calculate the means and standard errors of these properties for 46 different lifetimes. The error bars using the means and their standard errors are drawn, and the straight solid lines are the best linear fit for the means. Both of the fitted lines in Figure 5(a) and Figure 5(b) have a positive slope, but that in Figure 5(c) is negative.

For quantifying the degree of correlation, we calculate the correlation coefficients between the 46 lifetimes and the means of these properties. The correlation coefficient between lifetimes and diameters is 0.83; that between lifetimes and intensities is 0.65; however, the correlation between lifetimes and velocities appears to be a negative relation with a correlation coefficient of –0.49. Taking the precision of mean into account, a weighted correlation is also adopted. We calculate the weight as the reciprocal of the standard error of the mean, and get the correlation coefficients of 0.86, 0.58 and –0.73, respectively. Both of the correlation coefficients are in close agreement.

Figure 5 and the two sets of correlation coefficients imply the presence of correlations between the lifetimes and these properties: the isolated GBPs that live longer tend to be larger, brighter and slower. The correlations between the lifetimes versus diameters and intensities also agree with

Abramenko et al. (2010) who used a data set with a cadence of 10 s and a pixel size of 0.0375″ from the New Solar Telescope at Big Bear Solar Observatory.

6 DISCUSSION

The evolution of isolated GBPs are quantified by dividing the life into both 5 or 10 stages. Results from both sets of calculations show the same evolution pattern. However, the differences in the mean values at the different stages are very slight. To test the significance of the differences in the means of distributions at the different stages, we perform a two-sample t-test. At the 5% significance level, the test results indicate that there are significant differences in means between the distributions of the first stage and the middle stage, and between the middle stage and the last stage for diameter, intensity and velocity, no matter whether we divide the lifetimes into 5 or 10 stages.

The differences between the maximum and minimum values for diameter, intensity and velocity of five stages are 0.048, 0.015 and 0.074 respectively, and of 10 stages are 0.072, 0.032 and 0.183, respectively. Though the evolution patterns are in concordance, it can be seen that the difference between the maximum and minimum values of 10 stages is higher. As an experiment, we attempt to merge the means of ratios from 10 stages into five groups. For instance, we merge the value of the first stage and that of the second stage into a group, third stage and fourth stage into a group, etc. We then calculate the average of each group. The averages for diameters of five groups are 0.975, 1.017, 1.021, 1.012 and 0.975; for intensity they are 0.988, 1.009, 1.010, 1.004 and 0.988; for velocity they are 1.04, 0.964, 0.947, 0.991 and 1.059, respectively. Obviously, the averages are very close to the value of five stages (Tables 1, 3 and 5) and the differences are slight. We also calculate the difference between the maximum and minimum values of merging results for size, intensity and velocity and they are 0.046, 0.022 and 0.112, respectively. Comparing with the difference between the maximum and minimum values of 5 and 10 stages, the values of the merged results are closer to those of the five stages. However, there are some differences. We believe the reason is that the samples from the five stages are not the same as those from the 10 stages. The experiment indicates that fractionizing the life into 10 stages could yield more variations. If we divide the life into more stages, the difference between the maximum and minimum value would be much higher and the variation would be more pronounced. Of course, that depends on how long the GBP persists.

Another notable aspect is that the lifetime follows an exponential distribution and a large number of GBPs are short-lived. For normalizing the lifetime, we have to exclude some short-lived GBPs. This results in reducing the sample statistic. To avoid that, the temporal resolution of the image sequence needs to be improved. The higher the temporal resolution is, the more GBPs will be included, and a more precise result of the evolution pattern will be obtained.

The quantification result obtained by the method of normalizing the lifetime with a sufficiently large amount of data demonstrates the evolution pattern of an isolated GBP's size, intensity and velocity. This not only confirms the reports of Muller & Roudier (1992) and Utz et al. (2009) regarding the intensity of GBPs, but also suggests there is an evolution pattern for size and velocity.

7 CONCLUSIONS

We study the evolution pattern of isolated GBPs in terms of their size, intensity and velocity using high-resolution image sequences from the SOT G-band. A quantification method based on lifetime normalization is proposed. The method consists of the following main steps: dividing the GBP's life into common stages, calculating and normalizing the arithmetic mean of each stage, and curve fitting the PDFs of the normalized mean values at each stage. By dividing the lives of isolated GBPs into five stages, the results obtained are, on average, as follows: the diameter is 166 km at the birth stage, and it rises until its peak of 173 km at the middle stage, and then decreases to 165 km until disappearance; the maximum intensity contrast changes from 1.012 to 1.027, then down to 1.011; however, the velocity shows an opposing trend: the velocity changes from 1.709 to 1.593 km s^{-1} and

then up to 1.703 km s^{-1}. These results confirm previous studies, and demonstrate that the evolution pattern is such that the GBP is small, faint and fast-moving at the birth stage, becomes big, bright and slow-moving at the middle stage, then gets small, faint and fast-moving again at the decay stage until its disappearance. Based on the experiment, we find that regardless of whether the lifetime is divided into 5 or 10 stages, the evolution pattern is unaffected. We also use a two-sample t-test to check for a difference between the distributions of isolated GBPs' properties of the different stages. The test results imply that there are significant differences in the means between the distributions of the first stage and the middle stage, and between the middle stage and the last stage.

Furthermore, we quantify the relationship between the lifetimes of isolated GBPs and their properties. The conclusion is that there are positive correlations between the lifetimes and sizes and between lifetimes and intensities with correlation coefficients of 0.83 and 0.65, respectively; however, a negative correlation exists between the lifetimes and velocities with a correlation coefficient of –0.49. We also consider the precision of the means and calculate the weight as the reciprocal of the standard error of the mean, then get weighted correlation coefficients of 0.86, 0.58 and –0.73, respectively. Both of the correlation coefficients are in agreement. It is possible to conclude that the longer the GBP lives, the bigger, brighter and slower it will be.

Our quantification results could shed light on the evolution of magnetic flux tubes and their interaction with granular plasma. We also believe that the quantification method of using normalized lifetimes could be applied to study the evolution pattern of other features in a solar image sequence, and even used in other fields.

Acknowledgements The authors are grateful to the Hinode team for the possibility to use their data. Hinode is a Japanese mission developed and launched by ISAS/JAXA, in collaboration with NAOJ as a domestic partner, and NASA and STFC (UK) as international partners. Scientific operation of the Hinode mission is conducted by the Hinode science team organized at ISAS/JAXA. This team mainly consists of scientists from institutes in the partner countries. Support for the post-launch operation is provided by JAXA and NAOJ (Japan), STFC (U.K.), NASA (U.S.A.), ESA and NSC (Norway). The authors are grateful for the support received from the National Natural Science Foundation of China (Grant Nos. 11303011, 11263004, 11163004 and U1231205), Open Research Program of the Key Laboratory of Solar Activity of the Chinese Academy of Sciences (No: KLSA201309) and the open fund of the Key Laboratory of Modern Astronomy and Astrophysics, Nanjing University, Ministry of Education, China.

References

Abramenko, V., Yurchyshyn, V., Goode, P., & Kilcik, A. 2010, ApJ, 725, L101

Berger, T. E., Schrijver, C. J., Shine, R. A., et al. 1995, ApJ, 454, 531

Berger, T. E., Loefdahl, M. G., Shine, R. S., & Title, A. M. 1998, ApJ, 495, 973

Bovelet, B., & Wiehr, E. 2003, A&A, 412, 249

Cranmer, S. R. 2002, Space Sci. Rev., 101, 229

Cranmer, S. R., & van Ballegooijen, A. A. 2005, ApJS, 156, 265

Crockett, P. J., Mathioudakis, M., Jess, D. B., et al. 2010, ApJ, 722, L188

de Wijn, A. G., Rutten, R. J., Haverkamp, E. M. W. P., & Sütterlin, P. 2005, A&A, 441, 1183

Feng, S., Ji, K.-F., Deng, H., Wang, F., & Fu, X.-D. 2012a, Journal of Korean Astronomical Society, 45, 167

Feng, S., Deng, L. H., Shu, G. F., Deng, H., Wang, F., Ji, K. F., 2012b, A Subpixel Registration Algorithm for Low PSNR Images, IEEE fifth International Conference on Advanced Computational Intelligence (ICACI) (*http://ieeexplore.ieee.org/xpl/articleDetails.jsp?arnumber=6463241*)

Feng, S., Deng, L., Yang, Y., & Ji, K. 2013, Ap&SS, 348, 17

Ichimoto, K., Tsuneta, S., Suematsu, Y., et al. 2004, in Society of Photo-Optical Instrumentation Engineers (SPIE) Conference Series, 5487, Optical, Infrared, and Millimeter Space Telescopes, ed. J. C. Mather, 1142

Keys, P. H., Mathioudakis, M., Jess, D. B., et al. 2011, ApJ, 740, L40
Keys, P. H., Mathioudakis, M., Jess, D. B., et al. 2013, MNRAS, 428, 3220
Klimchuk, J. A. 2006, Sol. Phys., 234, 41
Möstl, C., Hanslmeier, A., Sobotka, M., Puschmann, K., & Muthsam, H. J. 2006, Sol. Phys., 237, 13
Muller, R., & Roudier, T. 1992, Sol. Phys., 141, 27
Muller, R., Roudier, T., Vigneau, J., & Auffret, H. 1994, A&A, 283, 232
Nisenson, P., van Ballegooijen, A. A., de Wijn, A. G., & Sütterlin, P. 2003, ApJ, 587, 458
Sánchez Almeida, J., Márquez, I., Bonet, J. A., Domínguez Cerdeña, I., & Muller, R. 2004, ApJ, 609, L91
Suematsu, Y., Tsuneta, S., Ichimoto, K., et al. 2008, Sol. Phys., 249, 197
Utz, D., Hanslmeier, A., Möstl, C., et al. 2009, A&A, 498, 289
Utz, D., Hanslmeier, A., Muller, R., et al. 2010, A&A, 511, A39
Zhao, M., Wang, J. X., Jin, C. L., & Zhou, G. P. 2009, RAA (Research in Astronomy and Astrophysics), 9, 933